Ecotoxicology and Environmental Safety 180 (2019) 509–516

Contents lists available at ScienceDirect

Ecotoxicology and Environmental Safety

journal homepage: www.elsevier.com/locate/ecoenv

Investigating the toxicities of different functionalized polystyrene nanoplastics on *Daphnia magna*

Wei Lin[a], Ruifen Jiang[b,**], Sizi Hu[a], Xiaoying Xiao[a], Jiayi Wu[a], Songbo Wei[a], Yaxin Xiong[a], Gangfeng Ouyang[a,c,*]

[a] KLGHEI of Environment and Energy Chemistry, School of Chemistry, Sun Yat-sen University, Guangzhou 510275, China
[b] Guangdong Key Laboratory of Environmental Pollution and Health, School of Environment, Jinan University, Guangzhou 510632, China
[c] College of Chemistry & Molecular Engineering, Center of Advanced Analysis and Computational Science, Zhengzhou University, Zhengzhou 450001, China

ARTICLE INFO

Keywords:
Nanoplastics (NPs)
Acute toxicity
Biomarkers
MAPK
Functional groups

ABSTRACT

Nanoplastics (NPs) spread widely with water and air current, and they can accumulate in aquatic organisms, even penetrating biofilms, which may cause persistent toxicity and potential hazards. This current study aimed to reveal the toxicological mechanism of different functionalized polystyrene (PS) NPs on *Daphnia magna* (*D. magna*) by investigating toxicity endpoints in individual level and biochemical level. In this study, acute toxicity, behavioral parameters and biomarker responses of *D. magna* was measured in the exposure of different functionalized PS NPs (plain PS, PS-p-NH_2, PS-n-NH_2 and PS-COOH). The results indicated that when exposed to the plain PS, ROS induction would activate MAPKs, thereby causing lethality and adverse behavior effects on *D. magna*; while the functionalized PS NPs were less toxic than the plain PS, especially for PS-p-NH_2 which was severely flocculated after exposure, thus showing no immobilization at the investigated concentrations. Also, the antioxidant system was mainly stimulated due to the direct interaction with the cell surface receptor, which was different from the plain PS. Consequently, this work suggests significant effects of functional groups on NPs for environmental toxicity studies, and provides a better understanding of the toxicological mechanism on the toxicity of PS NPs toward *D. magna*.

1. Introduction

Over the last few decades, the growing production of plastics has resulted in a marked increase in the disposal of plastics. A large amount of plastics have been discarded into the environment on a global scale, leading to the estimation that at least 250,000 tons have contaminated the global marine water (Eriksen et al., 2014), and most of the particles were less than 10 mm in size (Mattsson et al., 2015a). Under the force of nature, these plastics may eventually break down into nanoplastics (NPs) with at least one dimension less than 1 μm (da Costa et al., 2016; Koelmans et al., 2015). NPs have been shown to be more toxic than the regular plastics because they spread more widely in water and air currents, accumulate in organisms, and even penetrate biofilms (Alimi et al., 2018; Jeong et al., 2018; Holland et al., 2016; Rist et al., 2017; Jort Hammer and Kraak, 2012). Although there are methodological difficulties in detecting and quantifying such small and carbon-based particles in complex environmental matrices, nano-sized plastics are expected to be as ubiquitous as its bulk counterparts (Alimi et al., 2018; Lin et al., 2018).

Evidence is accumulating that NPs have adverse effects on a wide range of aquatic organisms (Brandon et al., 2016; Besseling et al., 2017; Bergami et al., 2016; Grigorakis et al., 2017; Saquing et al., 2010; Sun et al., 2018). Compared with micro-sized plastics which can cause physical injury in the intestinal tract (Nelms et al., 2016), NPs could be more harmful because of its small-sized effect with large specific surface area and strong penetration property, like other engineering nanomaterials. Several studies have verified that the potential of NPs could be ingested by a variety of biota and they can affect their environmental behavior (Lin et al., 2019; Jiang et al., 2018), including locomotor performance (Pitt et al., 2018), ingestion behavior (Bergami et al., 2016), food chain (Chae et al., 2018), growth and reproduction (Mattsson et al., 2015b). Jeong et al. (2016) reported that exposure of the monogonont rotifers to polystyrene (PS) particles would decrease their growth rate, fecundity, and lifespan, while increase the reproduction time. Studies also found that smaller particles (0.05- and 0.5-μm in diameter) appeared to be more toxic than the bigger one (6-

* Corresponding author. KLGHEI of Environment and Energy Chemistry, School of Chemistry, Sun Yat-sen University, Guangzhou, 510275, China.
** Corresponding author.
E-mail addresses: jiangrf5@jnu.edu.cn (R. Jiang), cesoygf@mail.sysu.edu.cn (G. Ouyang).

https://doi.org/10.1016/j.ecoenv.2019.05.036
Received 12 April 2019; Received in revised form 10 May 2019; Accepted 12 May 2019

μm in diameter). Addition of dissolved organic matter (*e.g.* humic acid) would reduce the toxic effects on *Daphnia magna* (*D. magna*) (Oriekhova and Stoll, 2018; Wu et al., 2019), which indicated that the toxicity of NPs might be not only related to its size, but also its surface properties. Bergami et al. found that 40 nm anionic carboxylic PS NPs presented aggregates in the gut of brine shrimp larvae even at a low NP concentrations (5 mg L^{-1}), thereby impairing feeding, motility and molting behaviors; On the contrary, larvae exposed to 50 nm cationic amino PS NPs and transferred to clean water did not show neither aggregated in the gut nor NPs adsorbed at the surface of sensorial antennules and appendages (Bergami et al., 2016). González-Fernández et al. evaluated the effects of 100 nm amino and carboxylic PS NPs on oyster gametes, and indicated that adhesion of both NPs could result in cellular responses of oyster spermatozoa, as well as relative cell size and complexity. However, the intracellular ROS production mechanism was varying between amino PS NPs and carboxylic PS NPs, where a significant increase of ROS production was observed with the exposure of the carboxylic PS NPs but not with the amino PS NPs (González-Fernández et al., 2018). Although many studies have demonstrated the toxic effect of NP on different organism, few of them has systematically investigated the toxicological mechanism.

In this study, we attempted to explore the toxicological mechanism of NPs on aquatic organism. Considering the fact that the toxicity of NP can vary depending on surface properties, different functionalized PS latex nanoparticles including amine-, positively charged carboxylate- and negatively charged carboxylate-modified PS NPs were chosen. Also, among invertebrate organisms, *D. magna* plays an important role in the aquatic ecosystem as a link between producers and high trophic consumers (Chae et al., 2018). As one of the most sensitive lab organisms to the environmental conditions (*e.g.* temperature and salinity) and stressors (*e.g.* radiation and pollutants) (Alberdi et al., 1996), *D. magna* serves as a model organism for understanding the toxic effects of many pollutants in aquatic environment, and thus, it was selected in this study. Dose-response curves were first conducted to investigate the acute toxic effects of different functionalized PS latex nanoparticles on *D. magna*. Then, behavioral parameters (movement velocity, maximum acceleration, movement distances, etc.) and biomarker responses (reactive oxygen species (ROS), activities of antioxidants and mitogen-active protein kinases (MAPK)) of *D. magna* were analyzed to further explore the defense mechanisms. This work investigated the toxicity endpoints at individual level and biochemical level, thereby providing a better understanding of the toxicological mechanism of *D. magna* in response to PS NPs with different functional groups.

2. Materials and methods

2.1. NP characterization and instruments

Four types of PS nanoparticles with and without surface modification were used in this study. Three of them, the plain, amine- and carboxylate-modified PS NPs with declared dimensions of 100 nm, 50–100 nm and 300 nm, respectively, were purchased from Aladdin (Shanghai, China). They were referred to as plain PS, PS-n-NH_2 and PS-COOH, respectively. Another amine-modified PS NPs with a declared dimension of 110 nm were purchased from Thermo Scientific (Shanghai, China), and was named PS-p-NH_2. The characters “n” and “p” mean negatively charged and positively charged, respectively.

An EliteSizer Omni instrument (Brookhaven Instruments Corp., New York, USA) coupled with dynamic light scattering (DLS) with a 90° scattering angle was used for measuring hydrodynamic diameters of PS NPs; while the same instrument coupled with phase analysis light scattering (PALS) and multi-frequency measurement were used for measuring zeta potentials of the NPs with a laser doppler electrophoresis method (Wu et al., 2019).

2.2. Cultivation of D. magna

D. magna collected from School of Life Science, Sun Yat-sen University was used for this study (Luan, 2015). The organisms were fed with a certain amount of *Scenedesmus subspicatus* twice a day and maintained in the artificial culture medium (M7) recommended by OECD standards 202 (2004). They were cultured in a temperature-monitored illumination incubator (A1000, Conviron Corporation, Canada) with a 16:8 (light:dark) photoperiod at 20 ± 1 °C. In the following experiments, dissolved oxygen, pH and ammonia levels were monitored before and after each treatment (Lei Ci PHS-3E pen; Aquasonic test kit). The parameters were all in the normal range according to the OECD test guidelines 202 (2004).

2.3. Acute toxicity of PS NPs toward D. magna

Acute toxicity experiments of PS NPs were carried out in 20 mL glass vials following the OECD test guidelines 202 (2004). According to the results of preliminary tests, the concentrations of plain PS, PS-COOH, PS-n-NH_2 and PS-p-NH_2 in exposure suspensions were set at a range of 0–75 mg L^{-1},0–70 mg L^{-1}, 0–40 mg L^{-1} and 0–100 mg L^{-1}, respectively. The experimental set-up was the same as that in the previous paper (Lin et al., 2019). Briefly, an original suspension of PS NPs and a 10 mL culture medium were mixed in each vial. Then, five newborn *D. magna* (within 24 h after birth) were placed into each vial, and maintained in the same condition as mentioned above. Each experimental treatment was conducted in quadruplicate. The *D. magna* was exposed to the suspensions for 48 h without refreshing the exposure medium. During this time, the immobilization was recorded at 0, 24 and 48 h. Afterwards, the lethality of *D. magna* (LC_{50}) was calculated by a Boltzmann function with associated 95% confidence intervals (CI).

In the preliminary test, the highest concentration pre-set should result in 100% immobilization while the lowest concentration showed no observable effect during the exposure period, indicating that all the substances (the culture medium) in the control were biocompatible.

2.4. Effects of PS NPs on behavioral parameters of D. magna

Adult *D. magna* (21 days after birth) was used to study the toxic effects of PS NPs at individual level. Five *D. magna* were transferred into a 20 mL glass vial containing a 10 mL exposure suspension. The exposure concentrations of all the PS NPs (plain PS, PS-COOH, PS-n-NH_2 and PS-p-NH_2) were 1 mg L^{-1}, the possible highest concentration in water environment. After 48 h’ exposure, two randomly selected individuals from each vial were transported to a 6 well plate with culture medium (1 *D. magna*/well, 2 wells/treatment, each treatment was conducted in triplicate) of a DanioVision™ observation chamber (Noldus Inc., Wageningen, The Netherlands). It was a 25-min test in light where the first 10-min period is habituation, while the subsequent 15-min period is detection. Video data were recorded at a sample rate of 15 times/second by a high-speed infrared camera. An Ethovision XT software was employed for calculation.

2.5. Measurement of ROS and antioxidant enzymatic activities

ROS and antioxidant enzymatic activity including glutathione (GSH), superoxide dismutase (SOD), acetylcholine esterase (AChE) and malonaldehyde (MDA), in *D. magna* were measured to investigate the acute toxicity effects of PS NPs. Approximately 300 individuals were exposed to 2 L culture medium containing different PS NPs (plain PS, PS-COOH, PS-n-NH_2 and PS-p-NH_2) with a concentration of 1 mg L^{-1} for 48 h. After that, the samples were collected from each beaker to perform the experiments. Each experiment was conducted in triplicate. Protein content of *D. magna* for each treatment was determined by the dye-binding method (Bradford, 1976) using bovine serum albumin standard (0–200 μg BSA mL^{-1} PBS).

ROS was measured by a traditional method described in the previous paper (Kim et al., 2011). Briefly, *D. manga* were first homogenized in 0.32 mM sucrose (20 mM HEPES, 1 mM $MgCl_2$ and 0.5 mM PMSF), then centrifugated at 4 °C for 20 min with a rotation rate of 10,000 × *g*. After that, the supernatants were collected and reacted with H_2DCFDA for measurement where the developed fluorescence was 485 and 520 nm wavelength for emission and excitation, respectively (Thermo Scientific Co., Varioscan Flash, Waltham, MA, USA).

GSH measurement was conducted using glutathione assay kit (Sigma-Aldrich) following manufacturer's instructions. Enzymatic activities of AChE and SOD, as well as MDA content in *D. magna* were measured by diagnostic reagent kits (NJJC Bio Inc., Nanjing, China) following the manufacturers' instructions. The specific activities of AChE and SOD were expressed as units (U) of activity per mg of protein, while the MDA content was expressed as nmol mg^{-1} protein. Details were described in Text S1.

2.6. Expression level measurement of signaling pathway proteins

The effect of PS NPs on MAPK signaling pathways was evaluated by the Western blot analysis. According to the methods from literature (Wuk et al., 2016a, 2016b; Kim et al., 2016), *D. magna* was tested for the phosphorylation patterns of c-Jun-N-terminal kinase (JNK) and p38 using anti-rabbit-Tyr185 and anti-rabbit-MAPK. Briefly, the PS NPs-exposed *D. magna* was homogenized in lysis buffer (40 mM Tris–HCl (pH 8.0), 120 mM NaCl, 0.1% NonidetP40) containing protease inhibitor cocktail (Roche, South San Francisco, CA, USA) for total protein extraction. After a series of treatments (Text S2), the bolts developed were visualized by following the enhanced chemiluminescence procedures in manufacturers' instructions.

2.7. Statistical analysis

The data were processed with both Microsoft Excel and GraphPad Prism 5 (GraphPad Software, La Jolla, CA). All data were expressed as the mean ± 95% confidence intervals. The statistical differences in behavioral experiments and biomarker experiments between the control and treatment groups were evaluated by *t*-test and one-way ANOVA test, and significance level was 0.05. A Holm-Sidak's multiple comparisons test with a single pooled variance was used for all the data analysis.

3. Results

3.1. Acute toxicity effects of PS NPs exposure

The exposure suspensions were characterized and showed in Table 1. Compared with those in pure water, the particle diameters of all the negatively charged PS NPs slightly increased after the exposure experiments and zeta potentials approximately decreased by half. Exceptionally, after *D. magna* exposure, the PS-p-NH_2 suspension was strongly flocculated (Fig. S2) with a hydrodynamic diameter of 3704 ± 152 nm which was almost twenty times larger with the zeta potential close to zero (1.72 ± 0.61 mV).

Acute toxicity of the PS NPs was first tested in terms of lethality percentage (LC_{50}) of *D. magna* (Fig. 1). PS NPs exhibited significant functional group-dependent toxicity for *D. magna*. The LC_{50} data (with 95% confidence intervals) of the plain PS, PS-COOH and PS-n-NH_2 from the dose-effect curves were 5.24 (4.47–6.13), 20.2 (16.7–24.3) and 8.56 (7.32–10.0) mg L^{-1}, respectively. No observable toxic effect was found in the PS-p-NH_2 suspensions with concentration was up to 100 mg L^{-1}.

3.2. Effects of PS NPs on D. magna behavioral parameters

After exposure in the PS NPs suspensions for 48 h, *D. magna* activity was measured in light. Total distance moved (total distance *D. magna* moved over the 15-min observation period, cm), mean velocity (cm s^{-1}), maximum acceleration (maximum instantaneous acceleration of *D. magna* over the observation period, cm s^{-2}) and percentage of moving (a ratio of moving and not moving time, %) were detected in a 15-min period. As shown in Fig. 2, compared with the control group, there were significant negative effects of the plain PS and PS-n-NH_2 treatments on the individual behaviors ($p < 0.10$), but no significant effect was found for the PS-COOH and PS-p-NH_2 treatments.

3.3. ROS levels, GSH content and enzymatic activities of SOD, AChE, and MDA

Compared with the control group, the intracellular ROS significantly increased in *D. magna* exposed to the plain PS suspension, while remarkable reductions were observed for the functionalized PS NPs treatments (Fig. 3a; $p < 0.05$). GSH content of *D. magna* in different PS NPs suspensions corresponded to ROS level, and a similar pattern was also observed in the case of AChE activity (Fig. 3b; $p < 0.05$). However, the SOD and MDA activities of *D. magna* exposure in all the PS NPs with functional groups rose 99–307% and 69–79%, respectively. Especially, a significant increase in SOD activity was observed in a PS-p-NH_2 suspension, which was two times higher than the control group (Fig. 3b; $p < 0.05$).

3.4. Phosphorylation of MAPKs

To investigate the effects of PS NPs on MAPK signaling pathways, the phosphorylation status of p38 (p-p38) and c-Jun N-terminal kinase (p-JNK) in 1 mg L^{-1} PS NPs suspensions were analyzed after 48 h exposure. As shown in Fig. 4, compared with the control group, both p-p38 and p-JNK increased after exposure to plain PS, PS-COOH and PS-n-NH_2 to a variable extent. However, for PS-p-NH_2, p-p38 increased while p-JNK decreased. The performances in the MAPKs of *D. magna* can be linked with the intracellular ROS levels (Fig. 3a), and the toxic effects of PS NPs with different functional groups can be clarified.

4. Discussion

Though the hazards associated with micro-sized plastics to biota have been well characterized recently, the adverse effects of NPs were just taken into account in environmental plastic studies. This study investigated different toxicity endpoints of *D. magna* and revealed the

Table 1
Lethality of *D. magna* in different PS NP suspensions (the mean with 95% CI, n = 4); and the PS NPs exposure suspension characterization (the mean ± SD, n = 3).

	Plain PS	PS-COOH	PS-n-NH_2	PS-p-NH_2
LC_{50}/mg L^{-1}	5.24 (4.47–6.13)	20.2 (16.7–24.3)	8.56 (7.32–10.0)	> 100
PD[a] in water/nm	117 ± 1.36	273 ± 4.20	92.8 ± 0.96	193 ± 2.30
PD after exposure/nm	165 ± 1.69	357 ± 11.0	107 ± 1.51	3704 ± 152
ZP[b] before exposure/mV	−40.0 ± 0.79	−35.9 ± 4.17	−30.4 ± 2.03	18.5 ± 8.84
ZP after exposure/mV	−23.2 ± 5.20	−14.0 ± 3.02	−16.6 ± 3.55	1.72 ± 0.61

[a] PD is particle hydrodynamic diameter of the PS NP measured by DLS.
[b] ZP is zeta potential of the PS NP measured by PALS.

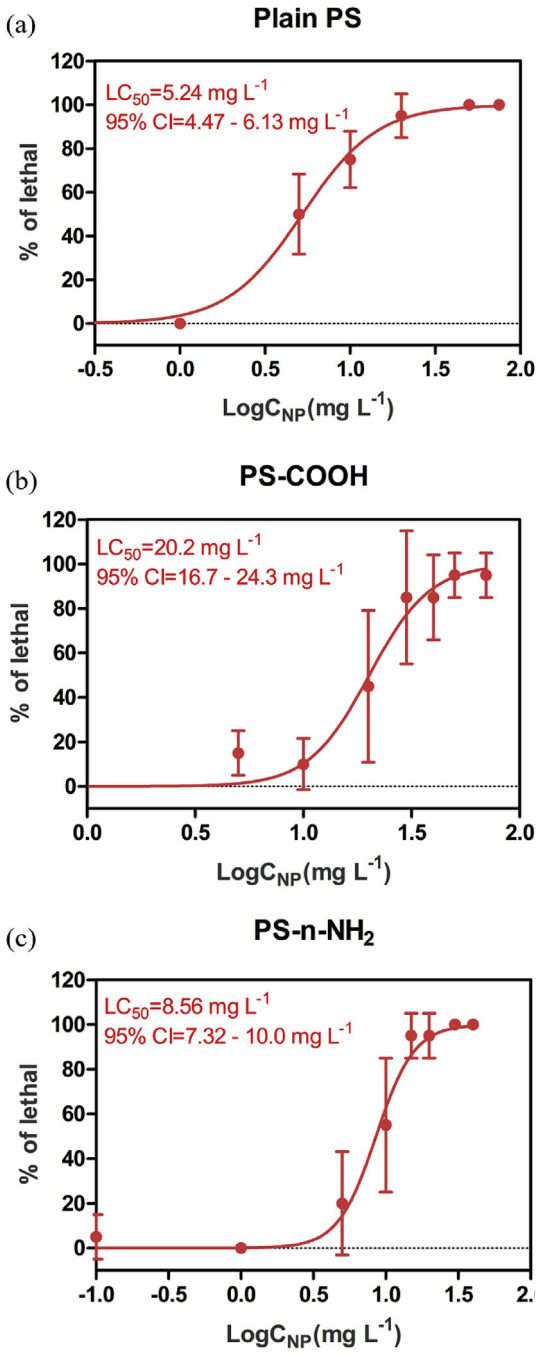

Fig. 1. Dose-response curves of (a) plain PS (100 nm), (b) PS-COOH (300 nm) and (c) PS-n-NH_2 (50–100 nm) on *D. magna* after 48 h exposure. No curve for PS-p-NH_2 (110 nm) because no observable toxic effect was found within the range of setting concentrations (up to 100 mg L^{-1}). Five *D. magna* samples were placed into each vial, and each experimental treatment was conducted in quadruplicate. The curves were fitted by the Boltzmann function: $y = y_2 + \frac{y_1 - y_2}{1 + 10^{(logLC50 - x) \cdot Hillslope}}$. Lethality of *D. magna* was the mean with 95% confidence intervals (n = 4).

toxicological process of different functionalized NPs. The following sections deeply discussed the results and considered the potential mechanisms associated with the behaviors at individual level and the biomarkers at molecular level.

In Table 1, the plain PS showed the most toxic effect on lethality of *D. magna*, followed by PS-n-NH_2, PS-COOH and PS-p-NH_2. As known, behavior is a crucial determinant for bioenvironmental adaptability assessment and is directly related to the lethality of organisms (Pitt et al., 2018). The acute toxicity results generally, but not perfectly, corresponded to the behavioral toxicities of *D. magna* in different PS NP suspensions (Fig. 2). Though the exposure concentrations of all the PS NPs in the behavioral experiments were set at 1 mg L^{-1}, the highest possible concentration in environmental water (Bergmann, 2015), the magnitude of lethality was different for each PS NP. The exposed concentrations account for 19.4%, 5.0%, 11.7% and less than 1.0% of the LC_{50} values in the plain PS, PS-COOH, PS-n-NH_2 and PS-p-NH_2 suspensions, respectively, which were roughly corresponded to the adverse effects on the *D. magna* behaviors. After 48 h of exposure, the particle diameters of plain PS and PS-n-NH_2 remained essentially unchanged, while those of PS-COOH and PS-p-NH_2 were 1.3 and 19.2 times larger than before, respectively (Table 1). Also, during the exposure process, the diameter of PS-COOH was always larger than those of plain PS and PS-n-NH_2. As reported, smaller microbeads were more "bioreactive" and should be more toxic than the larger ones (Jeong et al., 2016; Ma et al., 2016), so the different effects of the PS NPs might result from their different particle sizes. Rist et al. reported the accumulation amounts of 0.23 μg and 1.30 μg for each *D. magna* in a 100 nm PS suspension and a 2 μm PS suspension (1 mg L^{-1}), respectively (Rist et al., 2017). Since a particle volume of 2 μm PS was 8000 times as large as that of 100 nm PS, the number of accumulated particles of 100 nm PS were more than 1400 times as much of 2 μm PS for each *D. magna*. Particularly, no immobilization was observed in the PS-p-NH_2 suspension with a concentration of 100 mg L^{-1}, where a severe flocculation occurred after exposure (Fig. S2). It was demonstrated that the positively charged particle, PS-p-NH_2, would adsorb at the surface of brine shrimp larvae, and forced them to undergo multiple molting events (Bergami et al., 2016). Similarly, in this study, PS-p-NH_2 particles might impair the physiology (multiple molting) of *D. magna*, strongly bind with negatively charged shed skin cells of *D. magna* (Zhu et al., 2009), produce flocculation and destabilize the suspension system.

One of the main mechanisms behind the toxicity of NPs is related to the generation of intracellular ROS, which may have a negative effect on biological homeostasis in an organism (Magni et al., 2018; Bhattacharya et al., 2010). Compared with the control, being exposed to the plain PS significantly increased the ROS level of *D. magna* ($p < 0.05$), indicating that the plain PS induced ROS-related mitochondrial dysfunction (Wuk et al., 2016b), and that the integrity of mitochondrial membrane in *D. magna* decreased. PS NPs have been demonstrated as an inducer of ROS in organisms, which led to the antioxidant depletion and even deleterious effects on the behaviors and survival status (Pitt et al., 2018; Jeong et al., 2016, 2017). The induction of ROS would lead to oxidative stress and damage to the organism, specifically, lipid peroxidation indicated by MDA (Zhao and Zhu, 2016). As a final product of lipid peroxidation, MDA is closely related to oxidative damage on the lipid membranes of organisms. To resist disturbance, the nonenzymatic antioxidant defense system was activated where a chelating agent, GSH, was produced and chelated to ROS. Acting as a potent free-radical scavenger, GSH is responsible for maintaining the cellular redox state and protecting cells from oxidative stress (Habib et al., 2007). Therefore, MDA and GSH increases observed in the plain PS suspension suggested that the plain PS induced oxidative stress of *D. magna* and caused dysfunction of lipid membranes. Membrane dysfunction may also happen in a physical way where NPs directly interact with the membranes of the organisms and cause deleterious effects on biological processes like defense impairments (Jeong et al., 2018). There are evidences that PS NPs permeate easily into lipid membranes, alter membrane structure, affect membrane lateral organization and thereby interfere cellular function (Rossi et al., 2014). Also, the PS NPs (100-nm in diameter) were observed in *D. magna* body such as gut, antenna and even abdomen, indicating an uptake pathway through the epithelial cells of the skin or intestinal tract (Jiang et al., 2018).

In contrast, for the PS NPs with functional groups, the ROS levels

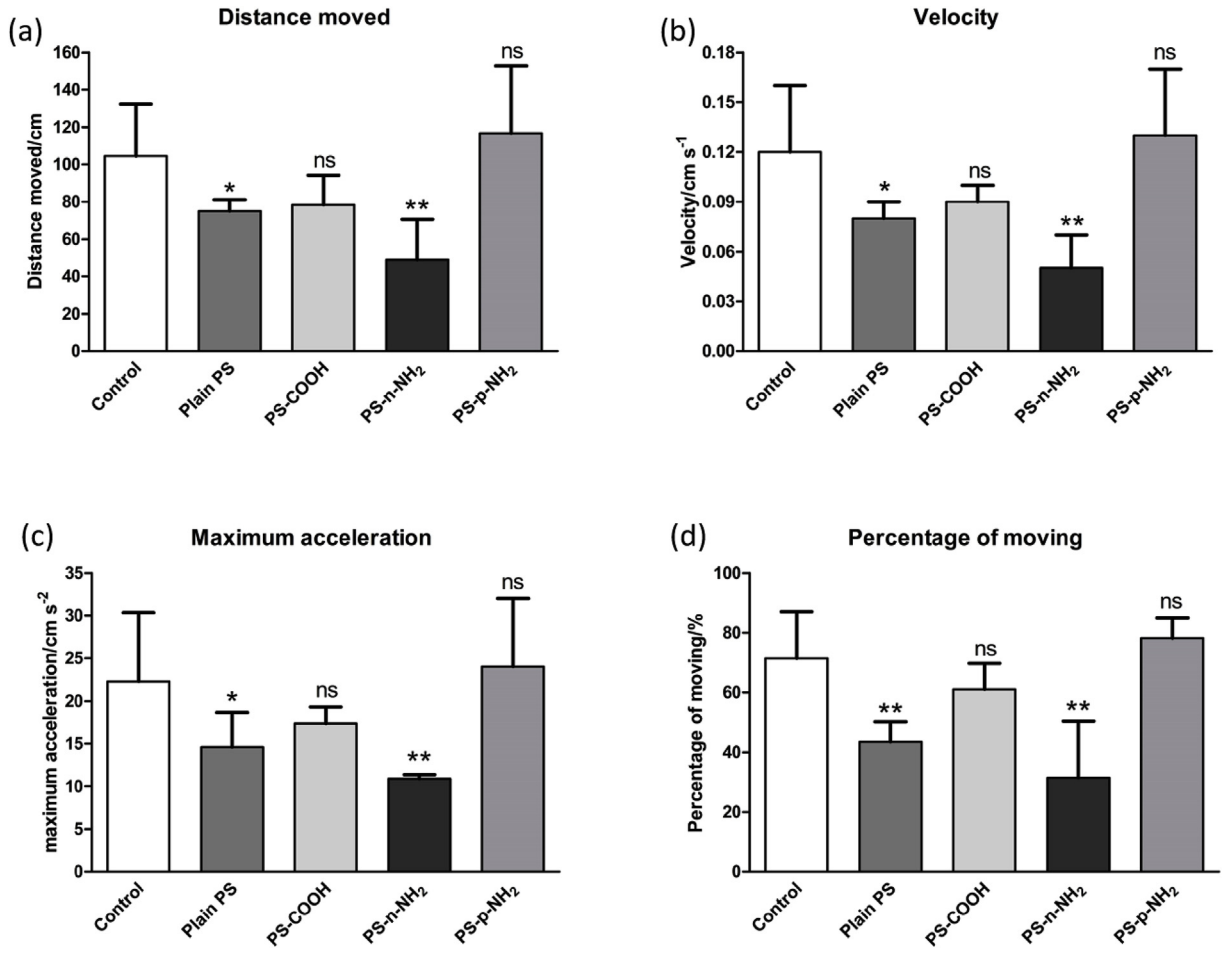

Fig. 2. Behavioral parameters in adult *D. magna* exposed to PS NPs with different functional groups after 48 h of exposure. (a) Total movement distance; (b) mean velocity; (c) maximum acceleration and (d) percentage of moving in a 15 min period. Error bar indicated the standard deviation (n = 6). Significant difference between the control and the treatment was represented as $^{*}p < 0.10$, $^{**}p < 0.05$.

and the GSH contents decreased. Normally, nanoparticles would trigger free radicals which reduce GSH by turning it to its oxidized form (glutathione disulfide, GSSG), and result in oxidative stress, apoptosis, sensitization to oxidizing stimuli, etc. (Rahman, 2007) Although the exact mechanism is unknown, it is perhaps due to the free radical scavenging property of the charged PS NPs. Cases of significant antioxidant depletion without ROS induction have been reported for some nanoparticles, such as multi-walled carbon nanotubes (Jeong et al., 2017) and metal NPs (Lin et al., 2017; May et al., 2018). Lipid peroxidation was observed with increases of MDA activities in response to these PS NPs, and induced modulation of antioxidant enzymes (*e.g.* SOD; Fig. 3b). Lu et al. illustrated that binding affinity between the NPs and lipid bilayer was a function of particle-cell wall interactions, and these interactions appeared to be electrostatic (Lu et al., 2015). Considering the cases above, reasons for modulation of antioxidant enzymes might be the low demand for the free radical scavenging or the unstable enzyme systems when exposed to the PS NPs. Nevertheless, compared with the control, GSH contents did not increase in response to modulation of antioxidant enzymes. It might because that *D. magna* had homeostatic ability to set up the detoxification mechanisms so as to defense and discharge these PS NPs (Zhao and Zhu, 2016).

AChE is an enzyme essential to the correct transmission of nerve impulses, so it confirms if the lack of avoidance in the behavioral assay is related with the neurotransmitter blockage. Many studies have clarified that inhibition of AChE activity had direct association with toxicological mechanisms of some contaminants such as pesticides (Sanchez-Hernandez et al., 2018; Guimarães et al., 2019), metals (Mkhinini et al., 2019) and manufactured materials (Chen et al., 2017). In this study, being exposed to plain PS suspension had no significant influence on AChE activity, while the functionalized PS NPs caused significant reductions in AChE activity (Fig. 3b), indicating deleterious effects in cholinergic neurotransmission and in nervous and neuromuscular function. It might be because both amino and carboxyl were hydrophilic and charged, that they tended to be easier to interact with the inorganic ions (Ca^{2+}, K^{+}, Na^{+}, Cl^{-}, etc.) of neurotransmitter, and interfere neurotransmission. Whereas AChE activities were not corresponded with the behavior of *D. magna* in different PS NPs, indicating that neurotransmission might not directly related to the apparent individual behavior. Also, AChE activity in different parts of an organism might react differently in response to external disturbance. For example, atrazine (1000 $\mu g\,L^{-1}$) reduced AChE activity in brain, thereby impairing defensive behaviors of zebrafish, while muscular AChE activity was not affected (Schmidel et al., 2014).

As one of the most thoroughly studied signal transduction systems, MAPK cascades have been verified to participate in a diverse array of cellular programs, including cell differentiation, movement, division and death (Schaeffer and Weber, 1999). MAPKs are responsible for apoptosis, inflammation and fibrosis, which have been proved to be related to PS NP toxicity in a few reports (Pinsino et al., 2017; Canesi et al., 2016). While ROS has the capacity to interfere with redox-sensitive signaling pathways, particularly with several MAPKs such as p38 MAPK, JNK and EPK (Jiang et al., 2013). When exposed to the plain PS suspension, both p38 and JNK phosphorylation (p-p38 and p-JNK) were activated and participated in signal transduction, resulting in the

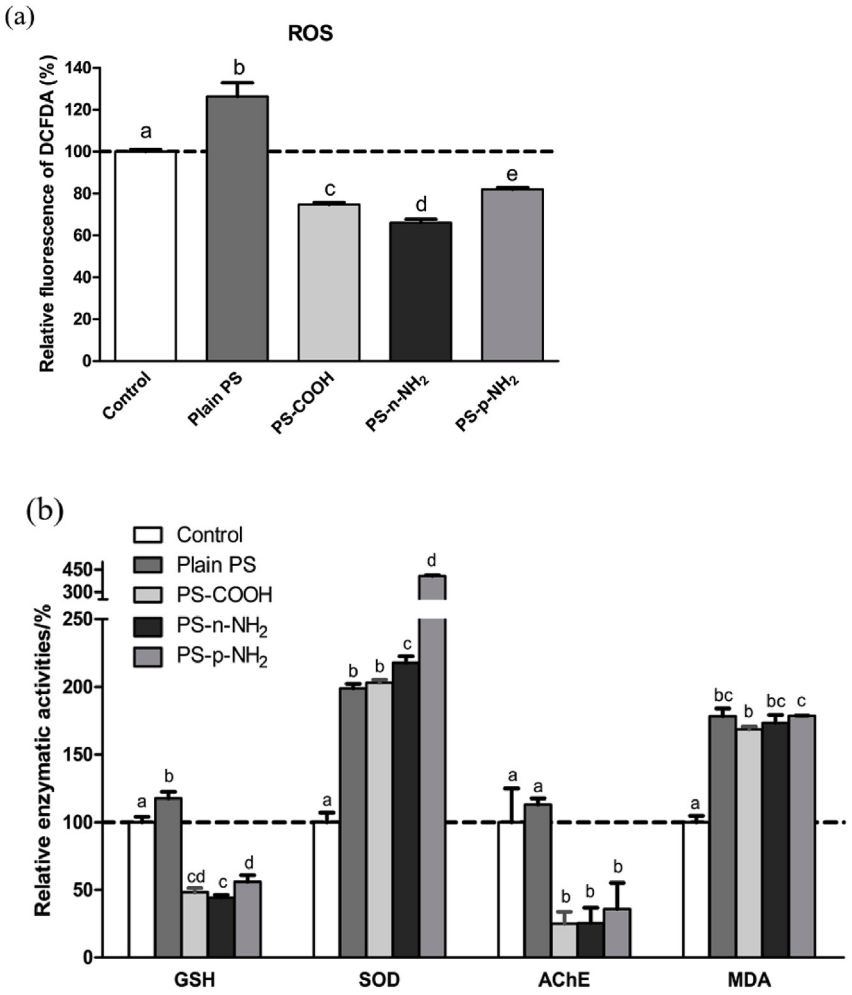

Fig. 3. Effects of 48 h exposure to PS NPs of different functional groups (plain PS, PS-COOH, PS-n-NH_2, and PS-p-NH_2) on ROS and antioxidant-related enzymes: (a) ROS levels; (b) GSH content, SOD, AChE and MDA activities. All the suspensions were 1 mg L^{-1}. Enzyme activities are represented as percentage of controls (n = 3). Different letters above columns indicate significant differences, defined as $p < 0.05$.

activation of p38 MAPK and JNK pathways, thereby causing oxidant stress reaction in *D. magna* (Fig. 4). The activation of MAPK pathways through p-p38 and p-JNK induction demonstrated that ROS is a key signal to activate MAPKs in the plain PS exposure, and an increase of ROS (Fig. 3a) is likely the major reason for toxicity. When exposed to the negatively charged PS NPs, PS-COOH and PS-n-NH_2, activation of MAPK pathways through p-p38 and p-JNK induction were observed without the increase of ROS. It may result from a direct interaction between the PS particles and the cell surface receptor (Kim et al., 2016), which causes the activation of p-p38 and p-JNK pathways. When exposed to the PS-p-NH_2 suspension, the increase of p-p38 MAPK and the decrease of p-JNK were observed with the reduction of ROS. It may be because of a direct interaction with the cell surface receptor, which causes an activation of p38 MAPK pathway, and a feedback suppression of p-p38 on JNK (Monick et al., 2006). A comparation between the negatively and positively charged PS NP showed that phosphorylation of p38 occurred in all the PS NPs-exposed *D. magna*, while JNK pathway was only activated by the negatively charged PS NPs-exposed *D. magna*. It is likely that p-JNK pathway could only be activated by neutral and negatively charged particles, while p-38 MAPK could be activated by all the PS NPs regardless of charge property (Haj et al., 2017; An et al., 2011). MAPK cascades activation is dependent on size, group, and charge in NPs-contained environment, and the PS NPs-induced adverse effects in *D. magna* take place through different signaling pathways.

5. Conclusions

This study revealed that acute toxicity to *D. magna* was related to functional groups of PS NPs. To be specific, the plain PS induced ROS production and activated MAPKs, thereby performing high acute toxicity towards *D. magna* and affecting their physiological behaviors. The PS-COOH and PS-n-NH_2 might interacted with cell surface receptor, activating MAPKs without ROS induction, and stimulating the antioxidant system. They were less toxic towards *D. magna* than the plain PS. Because of a severe flocculation, the PS-p-NH_2 had no adverse effects on the lethality and behaviors of *D. magna*, but the antioxidant system was stimulated due to the direct interaction with cell surface receptor. Also, our results indicated that AChE activity and p-JNK activation were related to the charge property of the PS NPs, but more experiments should be conducted for further verification. Through the exploration of the different functionalized PS NP effects, we linked the toxicity endpoints of organisms at individual level and biochemical level, and proposed a toxicological mechanism explaining the influence of functionalized PS NPs.

Conflicts of interest

There are no conflicts to declare.

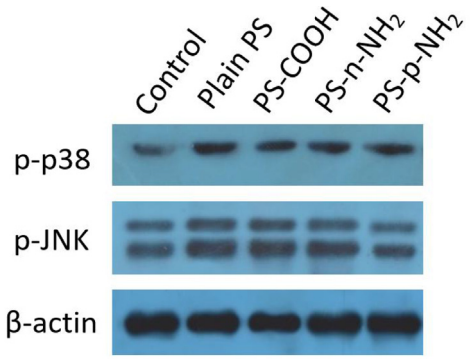

	Control	Plain PS	PS-COOH	PS-n-NH_2	PS-p-NH_2
p-p38	9640	16029	11351	12662	13602
β-actin	39783	38645	38525	40114	41638
p-p38/β-actin	0.24	0.41	0.29	0.32	0.33
p-JNK	31446	43187	44087	34858	26026
β-actin	3978	38644	38525	40114	41638
p-JNK/β-actin	0.79	1.12	1.14	0.87	0.63

Fig. 4. Effects of 48 h of exposure to PS NPs of different functional groups (plain PS, PS-COOH, PS-n-NH_2, and PS-p-NH_2) on phosphorylation of MAPK signaling proteins (n = 3). The proteins are represented as the optical density values for the target bands. All the suspensions were at a concentration of 1 mg L^{-1}.

Acknowledgements

The authors would like to acknowledge our funding sources, the National Natural Science Foundation of China (21777058, 21737006, 21477166, 21527813). In particular, the authors thank Qingjun Zhang for his help in behavioral experiments, and Xuekai Xu for the graphical editing and beautification of this article.

Appendix A. Supplementary data

Supplementary data to this article can be found online at https://doi.org/10.1016/j.ecoenv.2019.05.036.

References

Alberdi, J.L., Sáenz, M.E., Di Marzio, W.D., Tortorelli, M.C., 1996. Comparative acute toxicity of two herbicides, paraquat and glyphosate, to Daphnia magna and D. spinulata. Bull. Environ. Contam. Toxicol. 57 (2), 229–235.

Alimi, O.S., Farner Budarz, J., Hernandez, L.M., Tufenkji, N., 2018. Microplastics and nanoplastics in aquatic environments: aggregation, deposition, and enhanced contaminant transport. Environ. Sci. Technol. 52 (4), 1704–1724.

An, H.J., Kim, Y.J., Song, D.H., Park, B.S., Kim, H.M., Lee, J.D., Paik, S.G., Lee, J.O., Lee, H., 2011. Crystallographic and mutational analysis of the CD40-CD154 complex and its implications for receptor activation. J. Biol. Chem. 286 (13), 11226–11235.

Bergami, E., Bocci, E., Vannuccini, M.L., Monopoli, M., Salvati, A., Dawson, K.A., Corsi, I., 2016. Nano-sized polystyrene affects feeding, behavior and physiology of brine shrimp Artemia franciscana larvae. Ecotoxicol. Environ. Saf. 123, 18–25.

Bergmann, M., 2015. Marine Anthropogenic Litter. Springer.

Besseling, E., Quik, J.T.K., Sun, M., Koelmans, A.A., 2017. Fate of nano- and microplastic in freshwater systems: a modeling study. Environ. Pollut. 220, 540–548.

Bhattacharya, P., Lin, S., Turner, J.P., Ke, P.C., 2010. Physical adsorption of charged plastic nanoparticles affects algal photosynthesis. J. Phys. Chem. C 114, 16556–16561.

Bradford, M.M., 1976. A rapid and sensitive method for the quantitation of microgram quantities of protein utilizing the principle of protein-dye binding.pdf. Anal. Biochem. 72 (1–2), 248–254.

Brandon, J., Goldstein, M., Ohman, M.D., 2016. Long-term aging and degradation of microplastic particles: Comparing in situ oceanic and experimental weathering patterns. Mar. Pollut. Bull. 110 (1), 299–308.

Canesi, L., Ciacci, C., Fabbri, R., Balbi, T., Salis, A., Damonte, G., Cortese, K., Caratto, V., Monopoli, M.P., Dawson, K., et al., 2016. Interactions of cationic polystyrene nanoparticles with marine bivalve hemocytes in a physiological environment: role of soluble hemolymph proteins. Environ. Res. 150, 73–81.

Chae, Y., Kim, D., Kim, S.W., An, Y.J., 2018. Trophic transfer and individual impact of nano-sized polystyrene in a four-species freshwater food chain. Sci. Rep. 8 (1), 1–11.

Chen, Q., Yin, D., Jia, Y., Schiwy, S., Legradi, J., Yang, S., Hollert, H., 2017. Enhanced uptake of BPA in the presence of nanoplastics can lead to neurotoxic effects in adult zebrafish. Sci. Total Environ. 609, 1312–1321.

da Costa, J.P., Santos, P.S.M., Duarte, A.C., Rocha-Santos, T., 2016. Nano)plastics in the environment - sources, fates and effects. Sci. Total Environ. 566–567, 15–26.
Eriksen, M., Lebreton, L.C.M., Carson, H.S., Thiel, M., Moore, C.J., Borerro, J.C., Galgani, F., Ryan, P.G., Reisser, J., 2014. Plastic pollution in the world's oceans: more than 5 trillion plastic pieces weighing over 250,000 tons afloat at sea. PLoS One 9 (12), 1–15.
González-Fernández, C., Tallec, K., Le, N., Lambert, C., Gonz, C., Soudant, P., Huvet, A., Suquet, M., Berchel, M., Paul-pont, I., 2018. Cellular responses of Pacific oyster (Crassostrea gigas) gametes exposed in vitro to polystyrene nanoparticles. Chemosphere 208, 764–772.
Grigorakis, S., Mason, S.A., Drouillard, K.G., 2017. Determination of the gut retention of plastic microbeads and microfibers in goldfish (Carassius auratus). Chemosphere 169, 233–238.
OECD Guideline for the Testing of Chemicals. Daphnia sp. acute immobilisation test.
Guimarães, B., Maria, V.L., Römbke, J., Amorim, M.J., 2019. Multigenerational exposure of Folsomia candida to ivermectin - using avoidance, survival, reproduction, size and cellular markers as endpoints. Geoderma 337, 273–279.
Habib, G.M., Shi, Z.Z., Lieberman, M.W., 2007. Glutathione protects cells against arsenite-induced toxicity. Free Radic. Biol. Med. 191–201.
Haj, M., Wijeweera, A., Rudnizky, S., Taunton, J., Pnueli, L., Melamed, P., 2017. Mitogen- and stress-activated protein kinase 1 is required for gonadotropin-releasing hormone-mediated activation of gonadotropin α-subunit expression. J. Biol. Chem. 292 (50), 20720–20731.
Holland, E.R., Mallory, M.L., Shutler, D., 2016. Plastics and other anthropogenic debris in freshwater birds from Canada. Sci. Total Environ. 571, 251–258.
Jeong, C.B., Won, E.J., Kang, H.M., Lee, M.C., Hwang, D.S., Hwang, U.K., Zhou, B., Souissi, S., Lee, S.J., Lee, J.S., 2016. Microplastic size-dependent toxicity, oxidative stress induction, and p-JNK and p-p38 activation in the Monogonont Rotifer (Brachionus koreanus). Environ. Sci. Technol. 50 (16), 8849–8857.
Jeong, C.B., Kang, H.M., Lee, M.C., Kim, D.H., Han, J., Hwang, D.S., Souissi, S., Lee, S.J., Shin, K.H., Park, H.G., et al., 2017. Adverse effects of microplastics and oxidative stress-induced MAPK/Nrf2 pathway-mediated defense mechanisms in the marine copepod Paracyclopina nana. Sci. Rep. 7, 1–11.
Jeong, C.-B., Kang, H.-M., Lee, Y.H., Kim, M.-S., Lee, J.-S., Seo, J.S., Wang, M., Lee, J.-S., 2018. Nanoplastic ingestion enhances toxicity of persistent organic pollutants (POPs) in the monogonont rotifer Brachionus koreanus via multixenobiotic resistance (MXR) disruption. Environ. Sci. Technol. 52 (19), 11411–11418.
Jiang, Y., Zhang, H., Wang, Y., Chen, M., Ye, S., Hou, Z., Ren, L., 2013. Modulation of apoptotic pathways of macrophages by surface-functionalized multi-walled carbon nanotubes. PLoS One 8 (6), 1–15.
Jiang, R., Lin, W., Wu, J., Xiong, Y., Zhu, F., Bao, L.-J., You, J., Ouyang, G., Zeng, E.Y., 2018. Quantifying nanoplastic-bound chemicals accumulated in Daphnia magna with a passive dosing method. Environ. Sci. Nano 5, 776–781.
Jort Hammer, Michiel H., Kraak, S., 2012. J. R. P. Plastics in the marine environment: The dark side of a modern gift. In: Environmental Contamination and Toxicology. Springer Science + Business Media, pp. 1–44.
Kim, R., Rhee, J., Won, E., Lee, K., Kang, C., Lee, Y., Lee, J., 2011. Ultraviolet B retards growth, induces oxidative stress, and modulates DNA repair-related gene and heat shock protein gene expression in the monogonont. Aquat. Toxicol. 101 (3–4), 529–539.
Kim, D., Puthumana, J., Kang, H., Lee, M., Jeong, C., Han, J., Hwang, D., Kim, I., Wuk, J., Lee, J., 2016. Adverse effects of MWCNTs on life parameters, antioxidant systems, and activation of MAPK signaling pathways in the copepod Paracyclopina nana. Aquat. Toxicol. 179, 115–124.
Koelmans, A.A., Besseling, E., Shim, W.J., 2015. Chapter 12 nanoplastics in the aquatic environment. Critical review. In: Marine Anthropogenic Litter, pp. 1–447.
Lin, C.-X., Yang, S.-Y., Gu, J.-L., Meng, J., Xu, H.-Y., Cao, J.-M., 2017. The acute toxic effects of silver nanoparticles on myocardial transmembrane potential, INa and Ik1 channels and heart rhythm in mice. Nanotoxicology 11 (6), 827–837.
Lin, W., Jiang, R., Shen, Y., Xiong, Y., Hu, S., Xu, J., Ouyang, G., 2018. Effect of dissolved organic matter on pre-equilibrium passive sampling: a predictive QSAR modeling study. Sci. Total Environ. 635, 53–59.
Lin, W., Jiang, R., Xiong, Y., Wu, J., Xu, J., Zheng, J., Zhu, F., Ouyang, G., 2019. Quantification of the combined toxic effect of polychlorinated biphenyls and nano-sized polystyrene on Daphnia magna. J. Hazard Mater. 364, 531–536.
Lu, B., Smith, T., Schmidt, J.J., 2015. Nanoparticle-lipid bilayer interactions studied with lipid bilayer arrays. Nanoscale 7 (17), 7858–7866.
Luan, T., 2015. Surface-coated probe nanoelectrospray ionization mass spectrometry for analysis of target compounds in individual small organism. Anal. Chem. 87, 9923–9930.
Ma, Y., Huang, A., Cao, S., Sun, F., Wang, L., Guo, H., Ji, R., 2016. Effects of nanoplastics and microplastics on toxicity, bioaccumulation, and environmental fate of phenanthrene in fresh water. Environ. Pollut. 219, 166–173.
Magni, S., Gagné, F., André, C., Della Torre, C., Auclair, J., Hanana, H., Parenti, C.C., Bonasoro, F., Binelli, A., 2018. Evaluation of uptake and chronic toxicity of virgin polystyrene microbeads in freshwater zebra mussel Dreissena polymorpha (Mollusca: Bivalvia). Sci. Total Environ. 631–632, 778–788.
Mattsson, K., Hansson, L.A., Cedervall, T., 2015a. Nano-plastics in the aquatic environment. Environ. Sci. Process. Impacts 17 (10), 1712–1721.
Mattsson, K., Ekvall, M.T., Hansson, L.A., Linse, S., Malmendal, A., Cedervall, T., 2015b. Altered behavior, physiology, and metabolism in fish exposed to polystyrene nanoparticles. Environ. Sci. Technol. 49 (1), 553–561.
May, S., Hirsch, C., Rippl, A., Bohmer, N., Kaiser, J.-P., Diener, L., Wichser, A., Bürkle, A., Wick, P., 2018. Transient DNA damage following exposure to gold nanoparticles. Nanoscale 10, 15723–15735.
Mkhinini, M., Boughattas, I., Alphonse, V., Livet, A., Bousserrhine, N., Banni, M., 2019. Effect of treated wastewater irrigation in East Central region of Tunisia (Monastir governorate) on the biochemical and transcriptomic response of earthworms Eisenia andrei. Sci. Total Environ. 647, 1245–1255.
Monick, M.M., Powers, L.S., Gross, T.J., Flaherty, D.M., Barrett, C.W., Hunninghake, G.W., 2006. Active ERK contributes to protein translation by preventing JNK-dependent inhibition of protein phosphatase 1. J. Immunol. 177 (3), 1636–1645.
Nelms, S.E., Duncan, E.M., Broderick, A.C., Galloway, T.S., Godfrey, M.H., Hamann, M., Lindeque, P.K., Godley, B.J., 2016. Plastic and marine turtles: a review and call for research. ICES J. Mar. Sci. 73, 165–181.
Oriekhova, O., Stoll, S., 2018. Heteroaggregation of nanoplastic particles in the presence of inorganic colloids and natural organic matter. Environ. Sci. Nano 5, 792–799.
Pinsino, A., Bergami, E., Della Torre, C., Vannuccini, M.L., Addis, P., Secci, M., Dawson, K.A., Matranga, V., Corsi, I., 2017. Amino-modified polystyrene nanoparticles affect signalling pathways of the sea urchin (Paracentrotus lividus) embryos. Nanotoxicology 11 (2), 201–209.
Pitt, J.A., Kozal, J.S., Jayasundara, N., Massarsky, A., Trevisan, R., Geitner, N., Wiesner, M., Levin, E.D., Di Giulio, R.T., 2018. Uptake, tissue distribution, and toxicity of polystyrene nanoparticles in developing zebrafish (Danio rerio). Aquat. Toxicol. 194, 185–194.
Rahman, K., 2007. Studies on free radicals, antioxidants, and co-factors. Clinical Interventions in Aging, vol. 2. pp. 219–236.
Rist, S., Baun, A., Hartmann, N.B., 2017. Ingestion of micro- and nanoplastics in Daphnia magna – quantification of body burdens and assessment of feeding rates and reproduction. Environ. Pollut. 228, 398–407.
Rossi, G., Barnoud, J., Monticelli, L., 2014. Polystyrene nanoparticles perturb lipid membranes. J. Phys. Chem. Lett. 5 (1), 241–246.
Sanchez-Hernandez, J.C., Notario del Pino, J., Capowiez, Y., Mazzia, C., Rault, M., 2018. Soil enzyme dynamics in chlorpyrifos-treated soils under the influence of earthworms. Sci. Total Environ. 612, 1407–1416.
Saquing, J.M., Saquing, C.D., Knappe, D.R.U., Barlaz, M.A., 2010. Impact of plastics on fate and transport of organic contaminants in landfills. Environ. Sci. Technol. 44 (16), 6396–6402.
Schaeffer, H.J., Weber, M.J., 1999. Mitogen-activated protein kinases: Specific messages from ubiquitous messengers. Mol. Cell. Biol. 19 (4), 2435–2444.
Schmidel, A.J., Assmann, K.L., Werlang, C.C., Bertoncello, K.T., Francescon, F., Rambo, C.L., Beltrame, G.M., Calegari, D., Batista, C.B., Blaser, R.E., et al., 2014. Subchronic atrazine exposure changes defensive behaviour profile and disrupts brain acetylcholinesterase activity of zebrafish. Neurotoxicol. Teratol. 44, 62–69.
Sun, X., Chen, B., Li, Q., Liu, N., Xia, B., Zhu, L., Qu, K., 2018. Toxicities of polystyrene nano- and microplastics toward marine bacterium Halomonas alkaliphila. Sci. Total Environ. 642, 1378–1385.
Wu, J., Jiang, R., Lin, W., Ouyang, G., 2019. Effect of salinity and humic acid on the aggregation and toxicity of polystyrene nanoplastics with different functional groups and charges. Environ. Pollut. 245, 836–843.
Wuk, J., Won, E., Kang, H., Hwang, D., Kim, D., Kim, R., Lee, S., Lee, J., 2016a. Effects of multi-walled carbon nanotube (MWCNT) on antioxidant depletion, the ERK signaling pathway, and copper bioavailability in the copepod (Tigriopus japonicus). Aquat. Toxicol. 171, 9–19.
Wuk, J., Kang, H., Won, E., Hwang, D., Kim, D., Lee, S., Lee, J., 2016b. Multi-walled carbon nanotubes (MWCNTs) lead to growth retardation, antioxidant depletion, and activation of the ERK signaling pathway but decrease copper bioavailability in the monogonont rotifer (Brachionus koreanus). Aquat. Toxicol. 172, 67–79.
Zhao, Q., Zhu, L., 2016. Effect of humic acid on prometryn bioaccumulation and the induction of oxidative stress in zebrafish (Danio rerio). RSC Adv. 6 (20), 16790–16797.
Zhu, X., Zhu, L., Chen, Y., Tian, S., 2009. Acute toxicities of six manufactured nanomaterial suspensions to Daphnia magna. J. Nanoparticle Res. 11 (1), 67–75.